inter.noise 2014
MELBOURNE AUSTRALIA
16-19 NOVEMBER

Manipulation of source width based on sound field reproduction

Jung-Min Lee[1]; Jung-Woo Choi[2]; Yang-Hann Kim[3]

[1-3] Center for Noise and Vibration Control (NOVIC), Department of Mechanical Engineering, Korea Advanced Institute of Science and Technology (KAIST), Korea

ABSTRACT

In this study, a method is proposed to generate an extended virtual source enabling the extension of the perceived source width. In various auditory scenes, a sound source delivers the sensations of its size and location. The perceived source width is a spatial auditory impression related to the source size. Among the source width attributes, individual source width (ISW) is defined as the perceived width of an individual sound source disregarding a room effect. Accordingly, in representing a virtual source containing the size attribute, it is required to manipulate ISW as well as localization. The perceived source width is inversely proportional to the similarity of the listener's ear signals. The dissimilar pressures at both ears can be generated by randomizing the spectral phase distributions. In this paper, it attempts to produce the randomized phase distributions in a large area based on the sound field reproduction. To achieve this goal, a target sound field is designed such that the radiation pattern is randomly changed with respect to frequency. A direct solution for reproducing the designed field is then derived in terms of integral approach. Simulation results show that the proposed method can manipulate the perceived source width over a large area.

Keywords: Perceived source width, sound field reproduction
I-INCE Classification of Subjects Number(s): 74.9

1. INTRODUCTION

In room acoustics, spatial impression denotes "acoustical sensation of space", which is induced by the reflected waves reaching from different directions (1). However, such expression is not clear to describe various spatial attributes of a sound source placed in a room. Several researchers attempted to classify the spatial sensation, in terms of the increasing size of the sound source and the feeling of being enveloped by the ambient sound. They divided the spatial impression into two categories: apparent source width (ASW) and listener envelopment (LEV) (2-3). ASW is described as "the perceived width of the auditory image that is temporally and spatially fused with the direct sound image" (4), and LEV is defined as "the subjective impression of being enveloped by the reverberant sound field" (5). While LEV is the sensation of environment, ASW is perceived from the fused attributes of the sound source and room.

According to the references (6-7), the perception of the spatial attributes is caused by lateral reflections. In particular, Barron (7) found that the early lateral reflection arrived within 80ms after a direct sound leads to ASW. The late reflection after 80ms gives LEV (8). Accordingly, the two spatial attributes can be quantified by measuring the influence of the reflections, which reduces the similarity of listener's ear responses. Keet (9) experimentally showed that the dissimilar waves arriving at the listener's two ears lead to the ASW, and hence the perceived source width is inversely proportional to the measured similarity of the ear responses. One representative measure is the interaural cross-correlation coefficient (IACC) as follows (10)

$$IACC = \max_{\tau} \left| \frac{\int_{t_1}^{t_2} p_l(t) p_r(t+\tau) dt}{\sqrt{\int_{t_1}^{t_2} p_l^2(t) dt \int_{t_1}^{t_2} p_r^2(t) dt}} \right|, \tag{1}$$

[1] jungminlee@kaist.ac.kr
[2] khepera@kaist.ac.kr
[3] yanghannkim@kaist.ac.kr

where $p_l(t)$ and $p_r(t)$ are the pressure signals at left and right ears. The integral range t_1 and t_2 are determined from 0 to about 80ms considering the early lateral reflections in the reverberant condition. The time offset τ between the two pressure signals is bounded within ± 1ms due to the average size of the head, which is also considered as the maximum interaural time difference (ITD). IACC inversely indicates the perceived source width within the range of 0~1.

However, such classification of the spatial impression cannot describe the spatial attributes related to an individual sound source excluding the room effect. In recent works, Mason and Rumsey (11) subdivided the meaning of the spatial impression into "the auditory perception of the location, dimensions, and other physical parameters of a sound source and the acoustic environment in which the source is located". In addition, Rumsey (12) suggested more specific description of the width attributes produced by a sound source in a room, such as individual source width (ISW), ensemble width and environment width. According to the Rumsey's definition, environment width is described as "the broadness of reflective environment within which individual sources are located". On the contrary, the ISW and ensemble width is the width sensation discriminated from the room-related attributes, unlike ASW. The former is defined as "the perceived width of an individual sound source" and the latter means "the overall width of a defined group of the individual sources". Among these, ISW is more focused on the width attribute of a single sound source, disregarding its reflected waves coming from the environment.

For the realistic synthesis of a virtual sound source containing the width attribute, therefore, it is needed to manipulate ISW as well as the perceived location of an individual sound source. In representing a virtual object using a virtual reality system, the coherent visual and auditory perspective in temporal and spatial characteristics is required. For example, as a virtual object approaches to the user, the visual and auditory source width should be extended, and vice versa. In addition, a holographic sound can lead to equal perception of ISW as well as localization at different listener positions. In this study, a virtual sound source that can provide the broad ISW over a large area is defined as an *extended source*.

To generate an extended source, sound field reproduction technique is employed in this study. Sound field reproduction system aims to physically recreate the pre-defined target sound field of a virtual source using a loudspeaker array. Previous works mostly focused on reproducing a monopole sound source having omni-directional radiation pattern. However, several attempts for representing an extended virtual source have been studied. Ahrens (13) proposed a sound field of the physically extended source in which only high order contributions remain. In addition, Choi (14) designed the radiation pattern based on the deterministic phase modulation of the sound field, which can produce the dissimilar signals at listener's ear positions. The proposed sound field by Choi can give the equal source width perception to multiple listeners and increase the source width in relation to the distance between the extended source and the listener. However, the solution for reproducing both target fields has not been proposed yet.

In this study, we propose a target sound field that can reduce IACC in a large listening region. A radiation pattern of the sound field is designed such that the similarity of left and right ear signals are reduced by randomizing the phase distribution in space. To achieve this goal, we introduce the radiation pattern that is randomly changed with respect to the frequency. We then derive the direct solution for reproducing the proposed target sound field based on the integral approach. The perceived source width is distinct when the listener located close to a sound source, and hence we aim to render the extended source in the region between the array and the listener.

2. DESIGN OF TARGET SOUND FIELD

2.1 Far-field formula of a target sound field

To generate the extended source, we start with designing its target sound field. The target sound field is proposed such that the dissimilar waves are produced at the listener's two ears. A basic idea comes from the source width extension using channel-based decorrelation technique. Several researchers (15-16) found that the uncorrelated input signals fed into the loudspeakers can reduce the IACC. To implement such input signals, a mono signal is filtered into the several replicas that have a low similarity each other but sound identically: decorrelation. This can be accomplished by utilizing all-pass filters that can adjust the phase distribution of the original signal. One representative way is to randomize the phase distributions (17).

By the same token, we attempt to design a sound field that can generate the randomized phase distributions at ear positions with the flat spectral magnitudes. To achieve this goal, we propose the radiation pattern that is randomly changed with respect to the frequency. Since a low degree of IACC is usually induced by the laterally incident waves, we don't need to consider the radiation pattern in elevation angle. Hence, the proposed radiation pattern is designed to be independent of the elevation angle. In addition, to avoid the coloration change, magnitude of the directivity should be flat with respect to the frequency. For simplicity, we adopt the far-field expression of the sound field: $1/r$ decaying field. Consequently, the designed target field is described by high order harmonics in azimuthal angle, which is randomly varied with respect to the frequency, as follows:

$$P_t(\vec{r}) \approx \frac{e^{ikr}}{r} e^{i\ell\phi}, \tag{2}$$

where ℓ denotes the integer that is randomly determined within $[-\mathrm{A}, \mathrm{A}]$ at each frequency, and ϕ indicates the azimuthal angle. The radiation pattern of Eq. (2) leads to the wave fronts emitting in a spiral pattern. A random integer ℓ means the order of the harmonics, and thus large ℓ leads to rapid variation of the phase distribution in space. To select ℓ with an equal probability, ℓ is defined as a uniform random variable. Note that the frequency dependency of ℓ is omitted for simplicity.

However, the proposed target field (Eq. (2)) may not be reproducible if the formula of Eq. (2) does not satisfy the wave equation. Accordingly, we should check whether or not the proposed field is a solution of the wave equation. A general solution can be expressed by the spherical harmonics expansion (for example, see 18) . That is,

$$P_t(r,\theta,\phi) = \sum_{n=0}^{\infty}\sum_{m=-n}^{n} a_{nm} h_n^{(1)}(kr) Y_n^m(\theta,\phi), \tag{3}$$

where a_{nm} indicates the expansion coefficient corresponding to the order of n and m. The spherical Hankel function $h_n^{(1)}(kr)$ describes the radial characteristic of the sound field, and $Y_n^m(\theta,\phi)$ denotes the spherical harmonics that is related to the angular radiation. We will derive a_{nm} of the proposed field (Eq. (2)).

Considering the far-field behavior of the proposed sound field, the spherical Hankel function is approximated by the far-field assumption as follows (19):

$$h_n^{(1)}(kr) \approx (-i)^{n+1} \frac{e^{ikr}}{kr}. \tag{4}$$

The condition for the far-field approximation of $h_n^{(1)}(kr)$ is given by (19)

$$kr \gg \frac{n(n+1)}{2}. \tag{5}$$

This represents that kr should be much larger than the order of n for assuming the $1/r$ decaying field. Inserting Eq. (4) to Eq. (3) gives to

$$\begin{aligned} P_t(r,\theta,\phi) &\approx \frac{e^{ikr}}{r}\sum_{n=0}^{\infty}\sum_{m=-n}^{n} a_{nm}\frac{(-i)^{n+1}}{k} Y_n^m(\theta,\phi) \\ &= \frac{e^{ikr}}{r}\sum_{n=0}^{\infty}\sum_{m=-n}^{n} b_{nm} Y_n^m(\theta,\phi), \end{aligned} \tag{6}$$

where b_{nm} substitutes for $a_{nm}(-i)^{n+1}/k$. From the equality between Eq. (6) and the proposed field (Eq. (2)), we can obtain the following expansion relation:

$$\sum_{n=0}^{\infty}\sum_{m=-n}^{n} b_{nm} Y_n^m(\theta,\phi) = e^{i\ell\phi}. \tag{7}$$

The coefficient b_{nm} can then be calculated by using orthogonality of the spherical harmonics. That is,

$$\begin{aligned} b_{nm} &= \int_0^{2\pi}\int_0^{\pi} e^{i\ell\phi} Y_n^m(\theta,\phi)^* \sin\theta d\theta d\phi \\ &= \left[\int_0^{2\pi} e^{i(\ell-m)\phi} d\phi\right]\left[\sqrt{\frac{(2n+1)}{4\pi}\frac{(n-m)!}{(n+m)!}}\int_0^{\pi} P_n^m(\cos\theta)\sin\theta d\theta\right]. \end{aligned} \tag{8}$$

Here, b_{nm} is given by the product of the two integrals in Eq. (8). In the first bracket, the integral with

ϕ can be derived as $2\pi\delta_{m\ell}$, which extracts the contribution of the order $m=\ell$ in Eq. (7). The remaining term can be calculated to (20)

$$\sqrt{\frac{(2n+1)}{4\pi}\frac{(n-m)!}{(n+m)!}}\int_0^{\pi} P_n^m(\cos\theta)\sin\theta d\theta$$

$$=\sqrt{\frac{(2n+1)}{4\pi}\frac{(n-m)!}{(n+m)!}}\times\begin{cases} 0, \quad n+m\ odd \\ \dfrac{2m}{n}\dfrac{[(n/2)!]^2(n+m)!}{\{(n-m)/2\}!\{(n+m)/2\}!(n+1)!}, \quad n\ even, m\ even \\ -\dfrac{\pi m}{n2^{2n+1}}\dfrac{(n+m)!(n+1)!}{[\{(n+1)/2\}!]^2\{(n-m)/2\}!\{(n+m)/2\}!}, \quad n\ odd, m\ odd \\ 2, \quad n,m=0, \end{cases} \tag{9}$$

which eliminates the θ dependency of the radiation pattern at all frequency. When we replace the result of Eq. (9) with R_{nm}, the expansion coefficient a_{nm} can be expressed as

$$a_{nm}=\frac{2\pi k\delta_{m\ell}}{(-i)^{n+1}}R_{nm}. \tag{10}$$

Consequently, the target sound field designed for the extended source can be physically realized at far field because it satisfies the wave equation. To verify the proposed sound field in terms of the perceived source width, we need to inspect IACC calculated from the proposed target field (Eq. (2)).

2.2 IACC of the target sound field

By definition, IACC is calculated from the head-related impulse responses, and hence the head scattering effect is contained on the IACC. To simplify the derivation of IACC, however, the free field assumption is applied. When the listener's head is faced in the direction of the extended source as depicted in Figure 1, the pressures generated at left and right ear positions are expressed as

$$\begin{aligned} P_l &\equiv P_t\left(r,\phi+\frac{\Delta\phi}{2}\right)\approx\frac{e^{ikr}}{r}e^{i\ell\left(\phi+\frac{\Delta\phi}{2}\right)}, \\ P_r &\equiv P_t\left(r,\phi-\frac{\Delta\phi}{2}\right)\approx\frac{e^{ikr}}{r}e^{i\ell\left(\phi-\frac{\Delta\phi}{2}\right)}, \end{aligned} \tag{11}$$

where the subscript l and r indicate the left and right ear locations. The variable $\Delta\phi$ denotes the spanned angle between the left and right ear positions which are denotes as $(r,\phi+\Delta\phi/2)$ and $(r,\phi-\Delta\phi/2)$, respectively. Accordingly, $\Delta\phi$ depends on the listener's head size d and the distance r from the extended source.

Since the ITD becomes zero for the listener heading the extended source (Figure 1), the cross-correlation function has a maximum value at $\tau=0$. Accordingly, IACC can be rewritten as

$$IACC=\left|\frac{R_{lr}(0)}{\sqrt{R_{ll}(0)R_{rr}(0)}}\right|. \tag{12}$$

where $R_{lr}(\cdot)$ denotes the cross-correlation function of the ear signals, and it is normalized by $R_{ll}(\cdot)$ and $R_{rr}(\cdot)$ which indicate the maximum values of the auto-correlation functions.

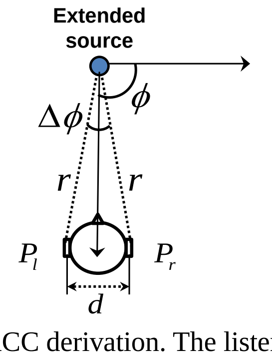

Figure 1 – Illustration of variables for IACC derivation. The listener's head with a diameter of *d* is located at a distance of *r* from the extended source.

Based on Wiener-Khinchin theorem (for example, see 21), the cross- and auto-correlation functions can be obtained by the inverse Fourier transform of the cross- and auto-spectral density functions. Since P_l and P_r are the random variables due to the random integer ℓ, we can estimate the spectral density functions as follows:

$$\hat{S}_{lr} = \frac{1}{T} E\left[P_l^* P_r\right], \hat{S}_{ll} = \frac{1}{T} E\left[P_l^* P_l\right], \hat{S}_{rr} = \frac{1}{T} E\left[P_r^* P_r\right], \tag{13}$$

where the finite time interval T denotes the time range that does not include the late reflections. Inserting Eq. (11) to Eq. (13), the spectral density functions are given by

$$\hat{S}_{lr} = \frac{1}{Tr^2} \frac{1}{2\mathrm{A}+1} \sum_{\ell=-\mathrm{A}}^{\mathrm{A}} e^{-i\ell\Delta\phi}, \hat{S}_{ll} = \hat{S}_{rr} = \frac{1}{Tr^2}, \tag{14}$$

where $1/(2\mathrm{A}+1)$ is the probability density function of the uniform random variable ℓ. The random integer ℓ is discretely distributed within the range of $[-\mathrm{A}, \mathrm{A}]$. By calculating the finite summation of the exponential function in Eq. (14) (22), the cross-spectral density function can be given by

$$\hat{S}_{lr}(\omega) = \frac{1}{Tr^2} \frac{1}{2\mathrm{A}+1} \frac{\sin\left\{(2\mathrm{A}+1)\dfrac{\Delta\phi}{2}\right\}}{\sin\left(\dfrac{\Delta\phi}{2}\right)} \equiv \frac{1}{Tr^2} \frac{\mathrm{csinc}_{(2\mathrm{A}+1)}(\Delta\phi)}{2\mathrm{A}+1}. \tag{15}$$

where $\mathrm{csinc}_{(2\mathrm{A}+1)}(\Delta\phi)$ denotes the circular sinc function (for example, see 23), which is normalized by $1/(2\mathrm{A}+1)$. Since the spectral density functions in Eqs. (14) and (15) are independent of the frequency, IACC can be rewritten without calculating the inverse Fourier transform of the spectral density functions, as follows:

$$IACC = \left| \frac{\mathrm{csinc}_{(2\mathrm{A}+1)}(\Delta\phi)}{2\mathrm{A}+1} \right|. \tag{16}$$

It is noteworthy that the derived IACC (Eq. (16)) is independent of the listener's angular position ϕ. This is advantageous for providing the perception of the source width to multiple listeners located at different ϕ for the fixed r. This behavior can be applied to the holographic sound of the extended virtual source.

The IACC formula of Eq. (16) depends on the random integer's bound A and the spanned angle $\Delta\phi$ that is varied with the distance between the extended source and the listener. If ℓ is zero at all frequencies (i.e., $\mathrm{A}=0$), IACC is calculated to one. Since zero ℓ leads to the monopole radiation, a point source will be perceived. In contrast, when ℓ is selected within a significantly broad range of $[-\mathrm{A}, \mathrm{A}]$ (i.e., large A), IACC will be reduced to zero. This means that the complex radiation patterns can increase the perceived source width. According to the derived IACC formula of Eq. (16), the major advantage of the proposed field is that the desired IACC can be produced by exploiting the appropriate A.

In addition, we can inspect the $\Delta\phi$ dependency on IACC. The extremely small $\Delta\phi$ leads to IACC of one, and this indicates that the extended source located far from the listener is perceived as a point source. However, if the extended source approaches near the listener ($\Delta\phi \approx \pi$), IACC converges to $1/(2\mathrm{A}+1)$, which is less than one due to $\mathrm{A} \geq 0$. Such observation gives the feasibility of the coherent auditory and visual perspective related to the width and distance. We will then reproduce the extended virtual source using a loudspeaker array.

3. REPRODUCTION OF TARGET SOUND FIELD

3.1 Derivation of driving function for a continuous line array

The perceived source width is distinct for a sound source located near the listener, and hence we aim to reproduce the proposed target field when the extended source is placed between the loudspeaker array and the listener. Since the Kirchhoff-Helmholtz (K-H) integral equation cannot describe the sound field from a sound source lying inside the listening area, we employ the modified integral equation (24):

$$\begin{aligned} P_a(\vec{r}) &\equiv P_t(\vec{r}) - P_{tr}(\vec{r})^* \\ &= \int_{S_s} \left[\nabla_s P_{tr}(\vec{r}_s)^* G(\vec{r}|\vec{r}_s) - P_{tr}(\vec{r}_s)^* \nabla_s G(\vec{r}|\vec{r}_s) \right] \cdot \vec{n}_s dS_s, \end{aligned} \tag{17}$$

where $P_t(\vec{r})$ denotes the target sound field diverging out of the extended source, and $P_{tr}(\vec{r})^*$ indicates the time reversed field converging into the extended source. Accordingly, the alternative field $P_a(\vec{r})$ represents the converging and diverging wave field. The free field Green's function $G(\vec{r}|\vec{r}_s)$ indicates the sound field emitted by a monopole control source located at $\vec{r}_s \in S_s$, and the inner product of its gradient and the surface normal vector $\vec{n}_s$ stands for the dipole field. Similar to the K-H integral, therefore, the modified integral equation (Eq. (17)) states that monopole and dipole sources distributed on a surface enclosing the listening area can generate the alternative field.

Considering a half infinite control surface as illustrated in Figure 2, the general integral equation (Eq. (17)) can be expressed as

$$P_a(\vec{r}) = \int_{-\infty}^{\infty} \int_{-\infty}^{\infty} \left[2\nabla_s P_{tr}(\vec{r}_s)^* G(\vec{r}|\vec{r}_s) \right] \cdot \vec{n}_s dx_s dy_s. \tag{18}$$

Applying the time reversal of the proposed target field to Eq. (18), this integral can be rewritten as

$$P_a(\vec{r}) = \int_{-\infty}^{\infty} \int_{-\infty}^{\infty} \left[2\nabla_s \left(\frac{e^{-ikR_v}}{R_v} e^{i\ell(\phi_v+\pi)} \right) \frac{e^{ikR_c}}{4\pi R_c} \right] \cdot \vec{n}_s dx_s dy_s, \tag{19}$$

where R_v denotes the distance between the extended source and each control source. The length R_c indicates the distance of the extended source from the control source. Since the proposed directional pattern is independent of the elevation angle, $e^{i\ell(\phi_v+\pi)}$ does not depend on y_s. Accordingly, Eq. (19) can be rewritten as

$$P_a(\vec{r}) = \int_{-\infty}^{\infty} e^{i\ell(\phi_v+\pi)} \left[\int_{-\infty}^{\infty} \left\{ -\left(ik + \frac{1}{R_v} \right) \vec{e}_{R_v} \cdot \vec{n}_s + \frac{i\ell}{R_v \sin\theta_v} \vec{e}_{\phi_v} \cdot \vec{n}_s \right\} \frac{e^{-ik(R_v - R_c)}}{2\pi R_v R_c} dy_s \right] dx_s, \tag{20}$$

where $\vec{e}_{R_v}$ and $\vec{e}_{\phi_v}$ denote the unit vectors in the direction of R_v and ϕ_v.

To render the extended source using a line array, it is required to reduce the surface integral of Eq. (20) to a line integral by approximating the integral with y_s. To accomplish this goal, we assume that the extended source is located at far distance from the array ($kR_v \gg 1$). This far-field assumption leads to

$$P_a(\vec{r}) \approx \int_{-\infty}^{\infty} e^{i\ell(\phi_v+\pi)} \left[\int_{-\infty}^{\infty} \left(-ik\vec{e}_{R_v} \cdot \vec{n}_s + \frac{i\ell}{R_v \sin\theta_v} \vec{e}_{\phi_v} \cdot \vec{n}_s \right) \frac{e^{-ik(R_v - R_c)}}{2\pi R_v R_c} dy_s \right] dx_s. \tag{21}$$

Such far-field source produces the pressure having smoothly varying magnitude distribution on the control surface. The integral around a stationary phase point can then contribute to total integral, because the rest part of the integral is canceled out due to the rapidly varying phase. Since the radiation pattern is independent of y_s, the stationary phase approximation (SPA) (for example, see 25) can be applied to the integral with y_s irrespective of the behavior of $b(\phi_v + \pi)$.

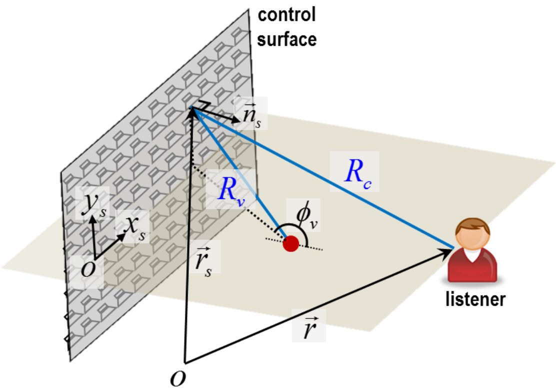

(a) for planar control surface

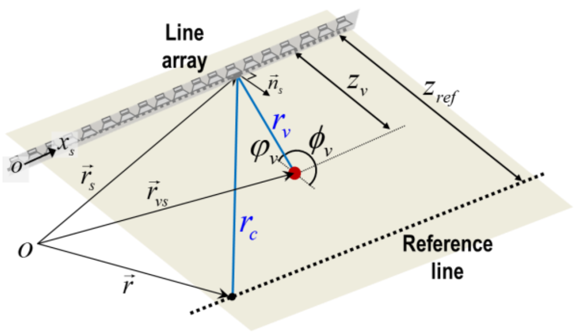

(b) for approximated line array

Figure 2 – Illustration of variables.

Considering the SPA which is defined by

$$\int_{-\infty}^{\infty} f(y)e^{i\Theta(y)}dy \approx f(y_0)e^{i\Theta(y_0)}\sqrt{\frac{2\pi i}{\Theta''(y_0)}}, \tag{22}$$

the magnitude and phase distribution of the integrand is given by

$$f(y_s) = \left(-ik\vec{e}_{R_v}\cdot\vec{n}_s + \frac{i\ell}{R_v\sin\theta_v}\vec{e}_{\phi_v}\cdot\vec{n}_s\right)\frac{1}{2\pi R_v R_c}, \Theta(y_s) = -k(R_v - R_c). \tag{23}$$

Here, the $1/R_v$ term leads to smoothly varying magnitude, and the phase distribution $-k(R_v - R_c)$ has a single stationary point. Assuming the extended source and listener are located at $y_s = y = 0$, the stationary phase point is placed at the same height ($y_0 = 0$). In addition, the distance R_v and R_c becomes $\sqrt{r_v^2 + y_s^2}$ and $\sqrt{r_c^2 + y_s^2}$, respectively (Figure 2). Accordingly, the magnitude and the second derivative of the phase at stationary phase point ($y_0 = 0$) are expressed as

$$f(y_0) = \left(-ik\vec{e}_{R_v}\cdot\vec{n}_s + \frac{i\ell}{r_v}\vec{e}_{\phi_v}\cdot\vec{n}_s\right)\frac{1}{2\pi r_v r_c}, \Theta''(y_0) = k\frac{r_v - r_c}{r_v r_c}. \tag{24}$$

By inserting Eq. (24) into Eq. (22), the far-field component (Eq. (21)) can be approximated to

$$P_a(\vec{r}) \approx \int_{-\infty}^{\infty}\left[e^{i\ell(\phi_v+\pi)}\left(ik\cos\varphi_v + \frac{i\ell}{r_v}\sin\varphi_v\right)\sqrt{\frac{2\pi i r_c r_v}{k(r_v - r_c)}}\frac{e^{-ik(r_v - r_c)}}{2\pi r_v r_c}\right]dx_s. \tag{25}$$

Here, $\cos\varphi_v$ and $\sin\varphi_v$ are equal to $-\vec{e}_{R_v}\cdot\vec{n}_s$ and $\vec{e}_{\phi_v}\cdot\vec{n}_s$, respectively (Figure 2(b)).

To extract the driving function of the monopole control source in Eq. (25), we rearrange the integrand as follows:

$$P_{a,f}(\vec{r}) \approx \int_{-\infty}^{\infty}\left\{2\sqrt{2\pi ik}\left(\cos\varphi_v + \frac{\ell}{kr_v}\sin\varphi_v\right)\sqrt{\frac{r_c}{r_c - r_v}}\frac{e^{-ikr_v}}{\sqrt{r_v}}e^{i\ell(\phi_v+\pi)}\right\}\frac{e^{ikr_c}}{4\pi r_c}dx_s, \tag{26}$$

where the formula in the parentheses becomes the driving function of the monopole control sources. However, since the driving function depends on the listener's position according to $r_c = |\vec{r} - \vec{r}_s|$, the derived solution cannot reproduce the target sound field at the multiple listening positions. For reproducing the target field in a region, we will modify the r_c-related term in the driving function based on SPA.

If the SPA again can be applied to the integral of Eq. (26), the reproduced field at a certain listening position $\vec{r}$ will be contributed by one control source located at the stationary phase point. Considering the multiple listening positions composing a line (i.e., reference line, 26), the target field on the reference line can be reproduced by superposing the contributions of the every control source. For the sound field reproduction on the reference line, therefore, r_c in the driving function should be defined as the distance between the listening position and the corresponding stationary phase point. We denote this distance as $r_{c,0}$. When the control source position x_s becomes the stationary phase point, the derivative of phase distribution with respect to x_s is equal to zero: $\partial k(r_c - r_v)/\partial x_s = 0$. From this relation, $r_{c,0}$ can be given by

$$r_{c,0} = \frac{z_{ref}}{\sqrt{1-\left(\sin\varphi_v + \frac{\ell}{kr_v}\cos\varphi_v\right)^2}}. \tag{27}$$

Note that $r_{c,0}$ is independent of the listening position x.

Consequently, the driving function can be expressed as

$$q(x_s) = 2\sqrt{2\pi ik}\left(\cos\varphi_v + \frac{\ell}{kr_v}\sin\varphi_v\right)\sqrt{\frac{r_{c,0}}{r_{c,0} - r_v}}\frac{e^{-ikr_v}}{\sqrt{r_v}}e^{i\ell(\phi_v+\pi)}, \tag{28}$$

where $\cos\varphi_v$ is equal to $-\partial r_v/\partial n_s$. The driving function of Eq. (28) includes the phase variation $e^{i\ell(\phi_v+\pi)}$ and gain compensation for the reference line $\sqrt{r_{c,0}/(r_{c,0} - r_v)}$ depending on ℓ.

3.2 Reproduction examples

The reproduction performance of the proposed driving function is examined using computer simulations. The reproduced field of the extended source located at (x_{vs}, z_{vs}) =(0m, 1m) is compared to the target field (Figure 3). For this example, the frequency was set to 1kHz. To simulate a continuous line array of control sources, a total of 2001 monopoles were distributed along the x axis with the constant spacing of 0.5cm (i.e., the line array was truncated to a length of 20m). The reference line was placed at 2m distance from the array (z_{ref} =2m). For $\ell = 3$, the real parts of the target field and reproduced field (Figure 3(a)) are depicted. The magnitude of the pressure fields are scaled such that the pressure at the center position of the reference line is equal to one. The result shows that the target field is reproduced in the region around and behind the reference line. However, the reproduced field cannot describe the radiation pattern of the target field at near field. This is due to the far-field assumption applied to the target field.

In order to quantify the accuracy of the reproduced field, we examine the relative error between the target and reproduced field, which is defined as

$$\varepsilon(\vec{r}) = 10\log_{10}\frac{\left|P_t(\vec{r}) - P_r(\vec{r})\right|^2}{\left|P_t(\vec{r})\right|^2}, \tag{29}$$

where $P_r(\vec{r})$ denotes the reproduced field. As depicted in Figure 3(a), the reproduction error is less than −20dB in the region of the reference line. From the result, we can conclude that the proposed solution can give the accurate reproduction of the extended source for $\ell = 3$ at reference line.

To evaluate the reproduction performance for large ℓ, the target field for $\ell = 10$ is reproduced as illustrated in Figure 3(b). The reproduced field looks identical to the target field around the center of the reference line, but the magnitude and phase differences between the two pressure fields can be seen in the other region. This result is quantified by the reproduction error distribution. Although the reproduction error is less than −20dB around the center of the reference line, the significantly large error is produced in the +x region of the reference line. This is because the rapid variation of the phase distribution due to large ℓ cannot be recreated by the waves having the wavelength of 1kHz frequency.

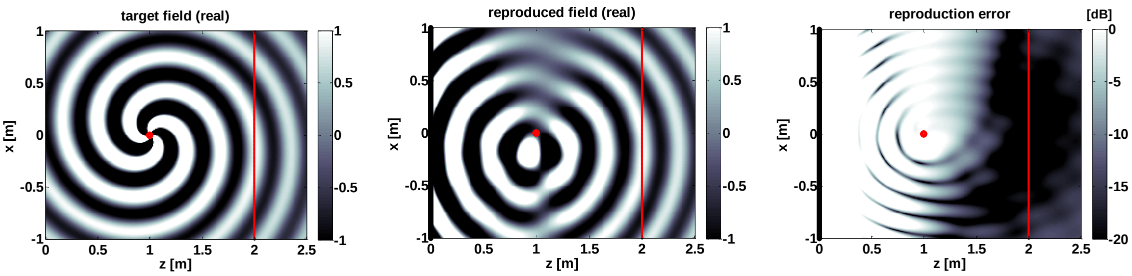

(a) reproduction results for ℓ =3

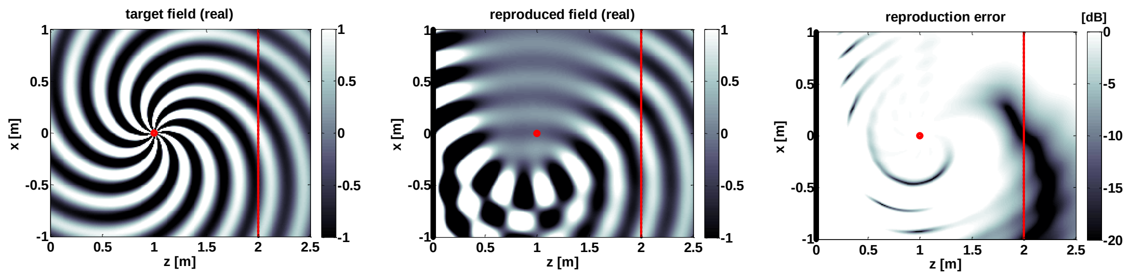

(b) reproduction results for ℓ =10

Figure 3 – Sound field reproduction by the proposed driving function ((x_{vs}, z_{vx}) =(0m,1m), f =1kHz).

4. EVALUATION OF IACC VARIATIONS

Since our goal is to provide the perceptual extension of the source width, IACC computed over the reproduced field is evaluated. We examine the variations of the reproduced IACC with respect to the distance of the extended source from listener (r) and the listener's angular position (ϕ) (Figure 4(a)). If the extended source approaches to the listener, IACC should be reduced. In addition, the reproduced field should produce equal IACC at all ϕ. For this example, the listener is placed at the center of the reference line (z_{ref}=3m). To avoid the artifact due to the spatial aliasing, a continuous array with the spacing of 0.5cm was used (L=20m). The IACC was calculated at the octave band of 1kHz center frequency, and A was set to 10.

As illustrated in Figure 4(b), the desired and reproduced IACCs are reduced as r decreases. However, the desired IACC curve tends to be oscillated in the small r region (r<0.7m) due to the near field effect. In particular, large reproduction error leads to the increasing IACC at near field. In addition, the reproduced IACC is independent of ϕ within only [-20°, 20°] due to large reproduction error in the range of $\phi > |20°|$, which is shown in Figure 4. From the results, it can be concluded that a line array can lead to the desired IACC behavior in the restricted region.

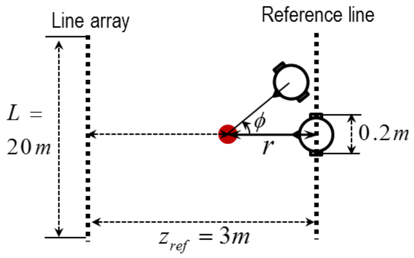

(a) Illustration of variables

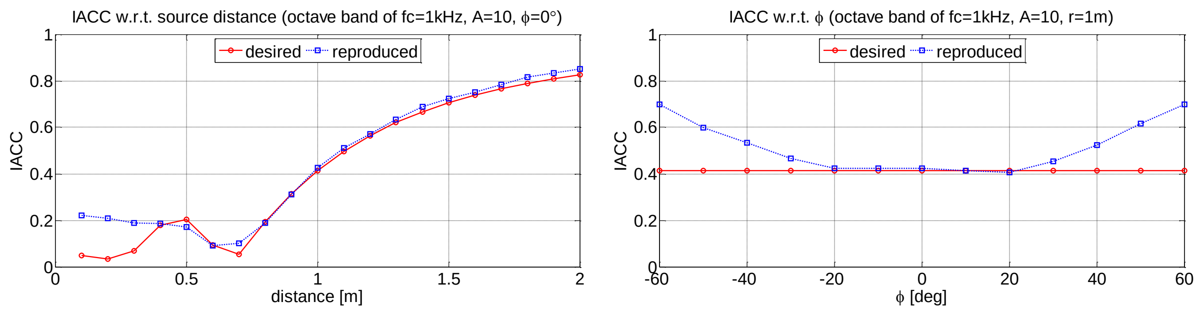

(b) comparison of IACC variations

Figure 4 – IACC variations with respect to the source distance and listener's angular position.

5. CONCLUSIONS

In this study, we proposed a method for rendering an extended virtual source that can provide the source width perception. To produce the desired source-width in a large listening area, sound field reproduction technique was applied. In addition, our goal was to give the same perspective as visual information: auditory source width should be extended for a nearby virtual source and reduced for a distant virtual source.

To reproduce such synthetic extended source, a target sound field was proposed. A radiation pattern of the extended source was designed to reduce IACC by decorrelating the pressures at any two points in a large listening area. The radiation pattern of the proposed field is randomly changed with respect to the frequency. We then derived the driving function for recreating the proposed target field. To obtain the driving function for a line array, the general integral equation for the planar control surface was reduced to a line integral by applying stationary phase approximation.

Simulations showed that the reproduction error decreased for a small value of ℓ. However, large reproduction error was produced in a region near the extended source, due to the far-field assumption. From the simulation results of the reproduced IACC, it was shown that the proposed method can mimic the behavior of the desired IACC in the restricted region.

ACKNOWLEDGEMENTS

This work was supported by the Ministry of Trade, Industry and Energy (MOTIE) grant funded by the Korea government (No. 10037244), and the BK21 (Brain Korea 21) project initiated by the Ministry of Education, and Unmanned Technology Research Center (UTRC) at Korea Advanced

Institute of Science and Technology (KAIST), originally funded by DAPA, ADD.

REFERENCES

1. Kuttruff H. Room acoustics. 4th ed. CRC Press; 2000. p. 222-223.
2. Morimoto M. and Maekawa Z. Auditory spaciousness and envelopment. Proc 13th Int. Congr. on Acoustics (ICA); 24-31 August 1989; Belgrade, Yugoslavia 1989. p. 215-218.
3. Bradley J. S. and Soulodre G. A. The influence of late arriving energy on spatial impression. J. Acoust. Soc. Am. 1995; 97(4): 2263-2271.
4. Morimoto M. and Maekawa Z. Effects of low frequency components on auditory spaciousness. Acta Acustica united with Acustica 1988; 66(4): 190-196.
5. Hidaka T., Beran L. L. and Okano T. Interaural cross-correlation, lateral fraction, and low- and high-frequency sound levels as measures of acoustical quality in concert halls. J. Acoust. Soc. Am. 1995; 98(2): 988-1007.
6. Marshall A. H. A note on the importance of room cross-section in concert halls. J. Sound Vib. 1967; 5(1): 100-112.
7. Barron M. The subjective effects of first reflections in concert halls-the need for lateral reflections. J. Sound Vib. 1971; 15(4): 475-494.
8. Bradley J. S. and Soulodre G. A. Objective measures of listener envelopment. J. Acoust. Soc. Am. 1995; 98(5): 2590-2597.
9. Keet W. V. The influence of early lateral reflections on the spatial impression. Proc 6th Int. Congr. on Acoustics (ICA); 21-28 August 1968; Tokyo, Japan 1968.
10. Damaske P. and Ando Y. Interaural crosscorrelation for multichannel loudspeaker reproduction. Acta Acustica united with Acustica 1972; 27(4): 232-238.
11. Mason R. and Rumsey R. An assessment of the spatial performance of virtual home theatre algorithms by subjective and objective methods. Proc 108th Audio Eng. Soc. Convention; 19-22 February 2000; Paris, France 2000. preprint 5137.
12. Rumsey F. Spatial quality evaluation for reproduced sound: terminology, meaning, and a scene-based paradigm. J. Audio Eng. Soc. 2002; 50(9): 651-666.
13. Ahrens J. and Spors S. Two physical models for spatially extended virtual sound sources. Proc 131st Audio Eng. Soc. Convention; 20-23 October 2011; New York, USA 2011. preprint 8483.
14. Choi J. -W. Extension of perceived source width using sound field reproduction systems. Proc 21st Int. Congr. on Acoustics (ICA); 2-7 June 2013; Montreal, Canada 2013.
15. Kurozumi K. and Ohgushi K. The relationship between the corss-correlation coefficient of two-channel acoustic signals and sound image quality. J. Acoust. Soc. Am. 1983; 74(6): 1726-1733.
16. Tohyama M. and Suzuki A. Interaural cross-correlation coefficients in stereo-reproduced sound fields. J. Acoust. Soc. Am. 1989; 85(2): 780-786.
17. Kendall G. S. The decorrelation of audio signals and its impact on spatial imagery. Computer Music Journal 1995; 19(4): 71-87.
18. Williams E. G. Fourier acoustics: spatial radiation and nearfield acoustical holography. London, Academic Press; 1999. p. 259.
19. Arfken G. B., Weber H. J. and Harris F. E. Mathematical methods for physicists: a comprehensive guide. 7th ed. Academic Press; 2012. p. 703.
20. Jepsen D. W., Haugh E. F. and Hirschfelder J. O. The integral of the associated Legendre function. Proc of the National Academy of Sciences of the United States of America; 1955; 41(9): p. 645-647.
21. Bendat J. S. and Piersol A. G. Random data: analysis and measurement procedures. 3rd ed. Wiley; 2000. p. 128-129.
22. Gradshteyn I. S. and Ryzhik I. M. Table of integrals, series, and products. edited by A. Jeffrey and D. Zwillinger. 6th ed. San Diego, Academic Press; 2000. p. 35.
23 Poletti M. The design of encoding functions for stereophonic and polyphonic sound systems. J. Audio Eng. Soc. 1996; 44(11): 948-963.
24. Choi J. -W. and Kim Y. -H. Integral approach for reproduction of virtual sound source surrounded by loudspeaker array. IEEE Trans. Audio, Speech, Lang. Process. 2012; 20(7): 1976-1989.
25. Bleinstein N. Mathematical methods for wave phenomena. New York, Academic Press; 1984, p. 77-81.
26. Verheijen E. N. G. Sound reproduction by wave field synthesis. Ph.D. thesis. Delft University of Technology, Delft, The Netherlands; 1997, p. 41.